



**HAL**  
open science

# Protonated hexaphyrin–cyclodextrin hybrids: molecular recognition tuned by a kinetic-to-thermodynamic topological adaptation

Stéphane Le Gac, Bernard Boitrel, Matthieu Sollogoub, Mickaël Ménand

## ► To cite this version:

Stéphane Le Gac, Bernard Boitrel, Matthieu Sollogoub, Mickaël Ménand. Protonated hexaphyrin–cyclodextrin hybrids: molecular recognition tuned by a kinetic-to-thermodynamic topological adaptation. *Chemical Communications*, 2016, 52 (60), pp.9347-9350. 10.1039/C6CC04276G . hal-01346462

**HAL Id: hal-01346462**

**<https://hal.sorbonne-universite.fr/hal-01346462>**

Submitted on 19 Jul 2016

**HAL** is a multi-disciplinary open access archive for the deposit and dissemination of scientific research documents, whether they are published or not. The documents may come from teaching and research institutions in France or abroad, or from public or private research centers.

L'archive ouverte pluridisciplinaire **HAL**, est destinée au dépôt et à la diffusion de documents scientifiques de niveau recherche, publiés ou non, émanant des établissements d'enseignement et de recherche français ou étrangers, des laboratoires publics ou privés.

## Protonated Hexaphyrin-Cyclodextrin Hybrids: Molecular Recognition Tuned by a Kinetic-to-Thermodynamic Topological Adaptation†

Received 00th January 20xx,  
Accepted 00th January 20xx

DOI: 10.1039/x0xx00000x

Stéphane Le Gac,<sup>\*a</sup> Bernard Boitrel,<sup>a</sup> Matthieu Sollogoub<sup>b</sup> and Mickaël Ménand<sup>\*b</sup>

www.rsc.org/

Protonation study of [26/28]hexaphyrin-capped cyclodextrins revealed a temperature controlled conformational transition of the cap. The hexaphyrin undergoes a rectangular-to-triangular shape-shifting which strongly modifies the shape of the confined environment featured by the hybrids, and ultimately affects the encapsulation of the counterions. It provides an attractive access to innovative allosteric host-guest systems.

Regulation processes in allosteric enzymes occur through complex stimuli-responsive conformational changes affecting ultimately the shape of the active site.<sup>1</sup> These sophisticated natural catalysts have constituted a blue print for the elaboration of artificial receptors and catalysts<sup>2</sup> integrating one or several major features of enzymes: a confined space, an allosteric control, and a dissymmetric active site.<sup>2a</sup> Self-assembled hosts/catalysts obtained through H-bonding or coordination processes have been efficiently designed, affording cage-like environments, some of them further exhibiting cavity shape reorganization.<sup>3</sup> However, due to the intrinsic “repetitive” and dynamic nature of self-assembly processes, these cavities are usually of high symmetry.<sup>4</sup> Conversely, covalent cages<sup>5</sup> offer the opportunity to produce dissymmetrical cavities in a more tuneable fashion, but the robustness of the covalent backbone reduces their conformational freedom and consequently their allosteric control. Therefore, triggering conformational changes important enough to affect the symmetry of a confined space in covalent host molecules deserves a particular attention. In this context, we have recently developed hybrid structures which associate a regular hexaphyrin(1.1.1.1.1.1) subunit to an  $\alpha$ -cyclodextrin one, namely HCDs.<sup>6</sup> In both [26] and [28]  $\pi$ -electron conjugated oxidation states, the hexaphyrin part

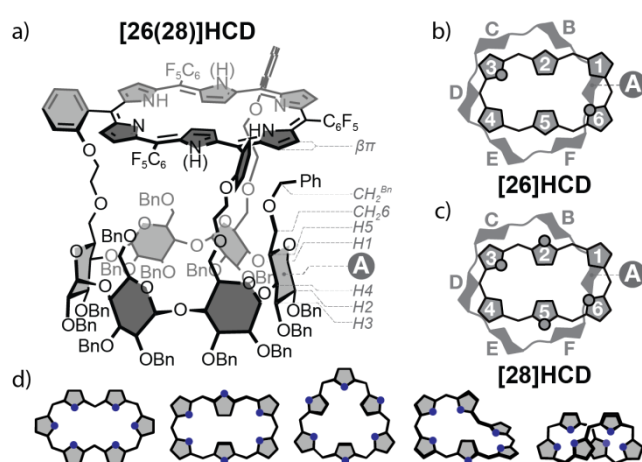


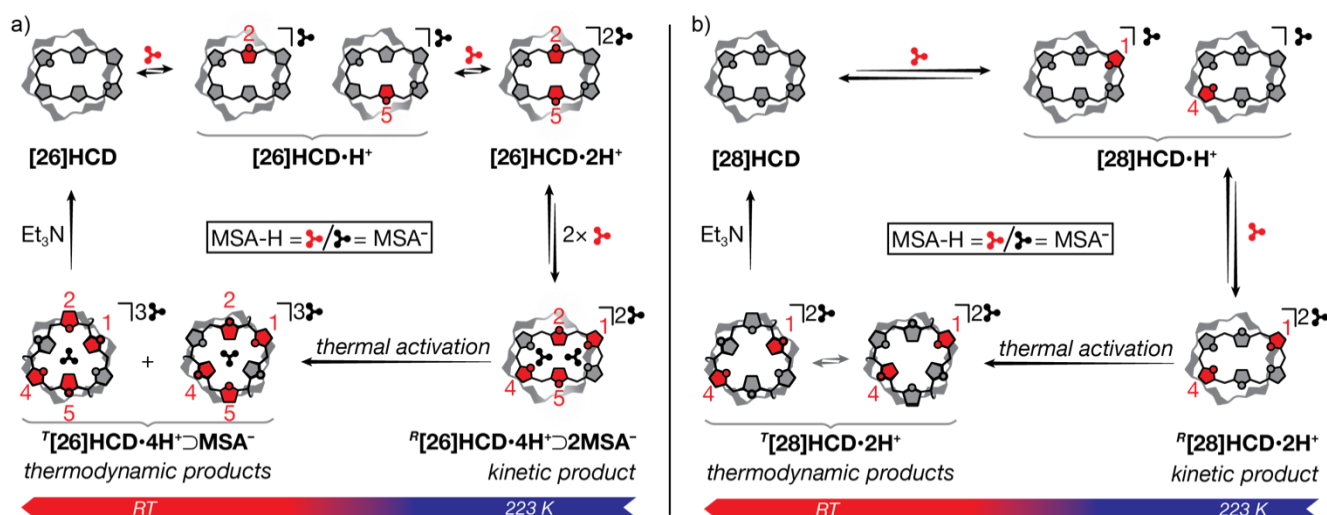
**Fig. 1** (a) Structure of [26]HCD and [28]HCD (NH in brackets) and their respective simplified representations (b and c). (d) General overview of the main conformations of hexaphyrin(1.1.1.1.1.1) macrocycle.

adopts a planar rectangular conformation with two central inverted pyrroles leading respectively to Hückel aromatic and antiaromatic compounds ([26]HCD/[28]HCD, Figure 1a-c). As the hexaphyrin cap protrudes over the “A” glucose unit of the cyclodextrin, the triple linkage defines an asymmetric space confined between the two subunits, which is thought of interest for the further hosting of molecules. Despite the triple covalent association, the hexaphyrin cap undergoes an inherent shape-shifting process between three degenerate rectangular conformations, through selective *in/out* pyrrole inversions.<sup>6</sup> This fluxionality prompted us to investigate the ability of the hexaphyrin cap to adopt other conformations, and how this would modify the global shape of the hybrid structure. Indeed, hexaphyrins can adopt different topologies (Figure 1d) whose stabilities are governed by various factors (substitution pattern, intramolecular hydrogen bonding, oxidation state, aromaticity, metal coordination, protonation state, solvent polarity...), leading to multiple possibilities for conformational switching.<sup>7</sup> For instance, stabilizing intramolecular hydrogen bonding interactions can be turned off by protonation of iminic pyrroles, allowing

<sup>a</sup> Institut des Sciences Chimiques de Rennes, UMR CNRS 6226, Université de Rennes 1, 263 av. du General Leclerc, 35042 Rennes cedex (France).  
E-mail: stephane.legac@univ-rennes1.fr.

<sup>b</sup> Sorbonne Universités, UPMC Univ Paris 06, and CNRS, Institut Parisien de Chimie Moléculaire (UMR CNRS 8232), 4 place Jussieu, 75005 Paris (France).  
E-mail: mickael.menand@upmc.fr.

† Electronic Supplementary Information (ESI) available: Experimental procedures and spectral data. See DOI: 10.1039/x0xx00000x



Scheme 1. Protonation pathways for (a) [26]HCD and (b) [28]HCD in CD<sub>2</sub>Cl<sub>2</sub> at 223 K and thermal activation at RT (protonated pyrroles colored in red).

twisting/untwisting events.<sup>8,9</sup> Herein, we show that protonated HCDs undergo a rectangular-to-triangular shape-shifting of the hexaphyrin cap through thermal activation, which deeply influences the encapsulation of counterions.

We first investigated the protonation behavior of [26]HCD and [28]HCD by UV-vis titration experiments with trifluoroacetic acid (TFA) and methanesulfonic acid (MSA) in CH<sub>2</sub>Cl<sub>2</sub> (ESI<sup>+</sup>). For both compounds, several transitions with clear isobestic points were observed, the stronger acid MSA leading more easily to higher degrees of protonation. While absorption maxima were overall redshifted, the Soret-like band shape was barely affected by the addition of acid, remaining sharp for the aromatic [26]HCD vs. ill-defined for the antiaromatic [28]HCD. This tends to indicate that the aromatic/antiaromatic characters of the macrocycles are preserved upon protonation. We then investigated the protonation of [26]HCD by NMR spectroscopy in CD<sub>2</sub>Cl<sub>2</sub> to gain further details into its conformational behavior. In contrast to experiments conducted with MSA at 298 K affording broad ill-defined spectra, those performed at 223 K led to four distinct states in slow exchange regime on the NMR timescale (Scheme 1a and Figure 2a-f): (i) the successive formation of mono- and diprotonated species, namely [26]HCD·H<sup>+</sup> and [26]HCD·2H<sup>+</sup>, was observed with *ca.* 1 and 2.5 equiv. of MSA (Figure 2b,c; green and yellow lines); (ii) between *ca.* 3 to 12 equiv. of MSA, [26]HCD·2H<sup>+</sup> disappeared leaving no clear signature, which presumably corresponds to an ill-defined mixture of triprotonated species; (iii) from 12 to 20 equiv. of MSA, a new well-defined signature emerged, and was attributed to a tetraprotonated state (Figure 2d; blue lines); (iv) upon standing the NMR tube at room temperature (RT, two successive 30 min periods), this signature was progressively converted into a 1:1 ratio of two other tetraprotonated species displaying NMR patterns of higher symmetry (Figure 2e,f; red lines). This indicates the existence of a kinetic product which transforms into a thermodynamic one, labeled respectively  $^R[26]HCD \cdot 4H^+ \rightleftharpoons 2MSA^-$  and  $^T[26]HCD \cdot 4H^+ \rightleftharpoons 2MSA^-$  (Scheme 1a; “R”/“T” stand for

“rectangular”/“triangular”, see below). It is noteworthy that addition of triethylamine (TEA) restored the initial rectangular conformation of [26]HCD.

These different signatures were analyzed through 2D NMR experiments. For the mono and diprotonated species, the highfield location of the four inner βπ, two inner NH and CH<sub>2</sub><sup>Bn</sup>(A) protons (Figure 2b,c) evidences rectangular hexaphyrin caps still protruding over the A glucose unit. Protonation occurs on the two central inverted pyrrole iminic nitrogen atoms (π2/π5, Scheme 1a), as attested by deshielded NH signals around 16.30 ppm for [26]HCD·H<sup>+</sup> and 16.40/16.75 ppm for [26]HCD·2H<sup>+</sup> in agreement with outward orientations (ESI<sup>+</sup>).

The subsequent protonation of π1 or π4 (triprotonated state) turned off one of the two “locking” intramolecular hydrogen bonds with π6/π3.<sup>7b</sup> The corresponding ill-defined NMR signature may thus account for more flexible hexaphyrins and/or for protonation competition between π1 and π4. Conversely, the perprotonation of the hexaphyrin cap restored a well-defined rectangular conformation (kinetic tetraprotonated product), as shown by the characteristic pattern that separates eight shielded inner protons (four βπ<sub>in</sub> [-3.62 to -5.01 ppm] and four NH<sub>in</sub> [-0.67 to -2.74 ppm]) from ten deshielded ones (eight βπ<sub>out</sub> [10.05 to 8.92 ppm] and two NH<sub>out</sub> [18.12 and 17.07 ppm]) (Figure 2d and SI). In addition, two highfield shifted singlets belonging to this species have been assigned through 2D HSQC NMR to the methyl groups of MSA counterions (δ<sup>[1H/13C]</sup> = -0.56/37.1 and -1.39/34.3 ppm, Figure 2d and ESI<sup>+</sup>). Their strong shielding (*ca.* 2.5 and 3.5 ppm compared to free MSA) indicates a position facing one of the two sides of the hexaphyrin mean plane. Furthermore, two distinct NOE correlation patterns (ESI<sup>+</sup>) in the crowded 4–2 ppm region (*i.e.* the cyclodextrin's primary rim and ethylenic spacer's protons) evidence their encapsulation between the linkers, in agreement with modeling studies of  $^R[26]HCD \cdot 4H^+ \rightleftharpoons 2MSA^-$  (Figure 3a,b). The perprotonated hexaphyrin cap, still projected over the A glucose unit, places one of the *endo*-MSA between unit A and π1/π6, the other

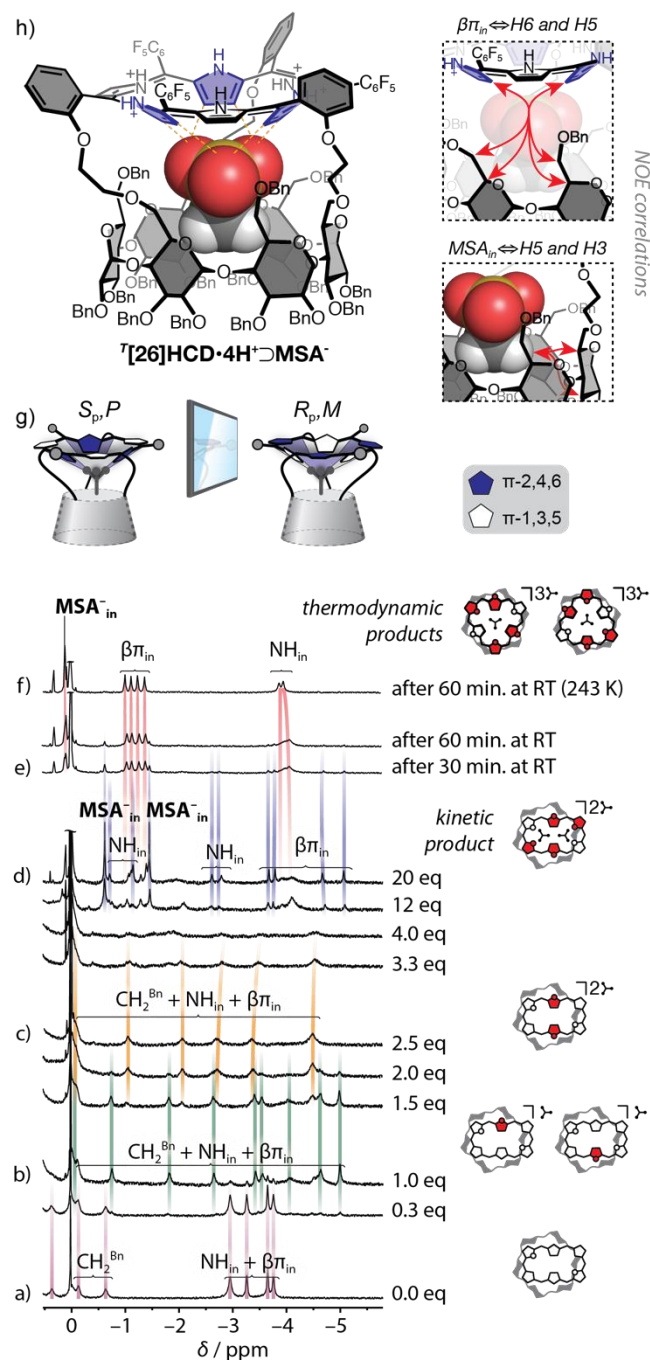


**Fig. 2.** From bottom to top:  $^1\text{H}$  NMR titration experiment of  $[\text{26}]\text{HCD}$  with  $\text{MSA}^-$  ( $\text{CD}_2\text{Cl}_2$ , 600 MHz, highfield region): (a-d) from 0 to 20 equiv., 223 K; (e) thermal equilibration at room temperature for 30 and 60 min, spectra then recorded at 223 K; (f) thermally equilibrated mixture, 243 K; (g) simplified representations of the triangular  $S_p,P$  and  $R_p,M$  diastereomers; (h) structure of the  $(S_p,P)$ - $[\text{26}]\text{HCD}\cdot\text{4H}^+\rhd\text{MSA}^-$  diastereomer (dashed lines indicate C-H...O hydrogen bonds).

one being close to the cyclodextrin axis (Figure 3a,b).

Upon thermal equilibration, the rectangular hexaphyrin cap underwent a conformational isomerization involving *in/out* inversions of three adjacent pyrroles, affording two triangular hexaphyrin caps as thermodynamic products ( $[\text{26}]\text{HCD}\cdot\text{4H}^+\rhd\text{MSA}^-$ , Figure 2e,f). Indeed, two  $C_3$ -symmetrical species were formed with either  $\pi$ 1,3,5 or  $\pi$ 2,4,6 oriented inward (Scheme 1a). They displayed two sets of

signals in both the highfield ( $\beta\pi_{\text{in}}$  [-0.92/-1.16 and -1.03/-1.28 ppm] and  $\text{NH}_{\text{in}}$  [-3.76 and -3.85 ppm], Figure 2f) and the downfield region ( $\beta\pi_{\text{out}}$  [10.34/9.69 and 9.85/9.21 ppm] and  $\text{NH}_{\text{out}}$  [16.14 and 16.16 ppm], SI), and the  $^{19}\text{F}$  NMR spectrum also showed two  $C_3$  symmetrical patterns (ESI $^+$ ). Formally, discrimination of the faces of a triangular hexaphyrin affords two opposite *meso*-substitution patterns such as “(AB) $_3$ ” and “(BA) $_3$ ”,<sup>10</sup> giving rise to an unprecedented planar chirality.<sup>11</sup> The triangular caps are indeed mirror images and not superimposable (Figure 2g;  $R_p/S_p$  descriptors, see the ESI $^+$ ) which, in addition, constitutes a new form of chirality supported by a CD.<sup>12</sup> Two diastereomers were thus obtained in the case of  $[\text{26}]\text{HCD}\cdot\text{4H}^+\rhd\text{MSA}^-$ , without chiral induction from the cyclodextrin subunit. Although not observed on the NMR time scale, selective *in/out* pyrrole inversions would allow interconversion of the two enantiomeric caps through an apparent exchange of the *meso*-substitution patterns (“(AB) $_3$ ”  $\leftrightarrow$  “(BA) $_3$ ”), which confers a dynamic character to this planar chirality (ESI $^+$ ).

This shape-shifting process is accompanied by a modification of the space confined between the primary rim of the cyclodextrin and its cap, which restricts the encapsulation to a single *MSA* counterion per diastereomer (singlets at 0.22 and 0.20 ppm, Figure 2f; 2D HSQC NMR:  $\delta[^{13}\text{C}] = 38.3$  ppm, ESI). NOE correlations observed in the complexes give some details about their geometry (arrows in the dashed box, Figure 2h): (i) correlations between the  $\beta\pi_{\text{in}}$  protons and both  $\text{CH}_26$  and  $\text{H5}$  protons of the cyclodextrin suggest a tilt of the inner pyrroles towards the cyclodextrin cavity which define a bowl shape conformation<sup>8b</sup> directing the convex face selectively inward; (ii) correlations between the  $\text{CH}_3$  protons of the *endo*-*MSA* and the cyclodextrin cavity ( $\text{H5}$  and  $\text{H3}$  [strong],  $\text{CH}_26$  [weak]) indicate a position at the entrance of the cyclodextrin cavity. These data agree with the stabilization of the *endo*-*MSA* through a network of six bifurcated C-H...O hydrogen bonds<sup>13</sup> between the sulfonate group and the tilted  $\beta\pi_{\text{in}}$  protons (Figure 2h), as recently observed in a X-ray structure of a *MSA*-protonated  $[\text{28}]\text{hexaphyrin}$ .<sup>8b</sup> Hence, the *MSA*-induced curvature of the triangular hexaphyrin introduces a “bowl” chirality (*M/P* descriptors, see the ESI $^+$ )<sup>11</sup> in addition to the planar one that lead to mirror images of the hexaphyrin caps, *i.e.* ( $S_p,P$ )- and ( $R_p,M$ )- $[\text{26}]\text{HCD}\cdot\text{4H}^+\rhd\text{MSA}^-$  (Figure 2g). The geometry optimization of the latter complex shows distances in good agreement with the observed NOE correlations (Figure 3c,d), and highlights the host-guest complementarity. Compared to the parent kinetic complex, the *endo*-*MSA* methyl group is located much closer to the cyclodextrin cavity (Figure 3b vs. 3d). Thus, while the driving force of the rectangular-to-triangular shape-shifting process may involve Coulombic repulsion between positive charges,<sup>8b</sup> it may also comprises a stabilization by the *endo*-*MSA* in the triangular complex. To the best of our knowledge, a stable triangular  $[\text{26}]\text{hexaphyrin}(1.1.1.1.1.1)$  has never been observed before.<sup>14</sup>

$^1\text{H}$  NMR investigations performed on the antiaromatic  $[\text{28}]\text{HCD}$  led to slightly different observations (Scheme 1b and ESI $^+$ ). Addition of 1 equiv. of *MSA* afforded the monoprotated

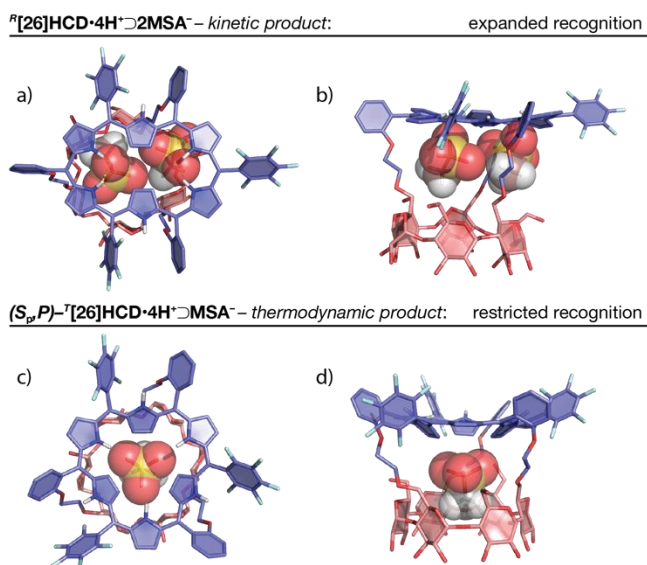


**Fig 3.** Top and side views of the optimized geometry of  $^R[26]\text{HCD}\cdot 4\text{H}^+\rightleftharpoons 2\text{MSA}^-$  (a,b) and  $(S,P)\text{-}^T[26]\text{HCD}\cdot 4\text{H}^+\rightleftharpoons \text{MSA}^-$  diastereomer (c,d) (Avogadro software, UFF parameters; benzyl groups and *exo*-MSA counterions were omitted for the modeling). *Endo*-MSA counterions are depicted in space filling.

$[28]\text{HCD}\cdot \text{H}^+$  displaying a broad  $C_1$  symmetrical spectrum with a strong deshielding of the hexaphyrin inner protons (22 to 33 ppm, four  $\beta\pi_{\text{in}}$  and three  $\text{NH}_{\text{in}}$ ) consistent with an antiaromatic rectangular conformation. Subsequent addition of MSA (2.5 equiv.) led to a new species characterized by a strongly broadened spectrum with chemical shifts spreading between *ca.* 50 and -2 ppm, suggesting a more planar rectangular conformation in the diprotonated state resulting in an impressive enhancement of the antiaromatic character ( $\text{ESI}^+$ ). Warming gradually from 223 K to 313 K revealed a slow exchange transition between  $^R[28]\text{HCD}\cdot 2\text{H}^+$  and a single species displaying an incomplete  $C_3$  symmetrical spectrum. 2D NMR analysis allowed assigning the “visible” signals to the cyclodextrin, the missing ones belonging to all protons located at and above the primary rim of the cyclodextrin (the hexaphyrin, the linkers and the  $\text{CH}_2\text{6-OBn}$ ). This suggests that the hexaphyrin part is involved in a coalescence phenomenon of large amplitude. Cooling back to 223 K did not allow to recover  $^R[28]\text{HCD}\cdot 2\text{H}^+$  but rather led to a global broadening of the spectrum indicating a probable intermediate exchange regime between two triangular conformations. Addition of TEA restored the initial rectangular conformation, attesting the preserved integrity of  $[28]\text{HCD}$ . Hence, in line with  $[26]\text{HCD}$ , the perprotonation of  $[28]\text{HCD}$  at low temperature led first to the antiaromatic rectangular kinetic product ( $^R[28]\text{HCD}\cdot 2\text{H}^+$ ) which upon thermal activation underwent a conformational rearrangement into the thermodynamic antiaromatic<sup>15</sup> triangular  $^T[28]\text{HCD}\cdot 2\text{H}^+$  (Scheme 1b). The rather ill-defined spectra of both  $^R[28]\text{HCD}\cdot 2\text{H}^+$  and  $^T[28]\text{HCD}\cdot 2\text{H}^+$  are probably the result of more dynamic structures in the  $[28]$   $\pi$ -electron oxidation state, preventing determination of the role of the MSA counterions in their stabilization.

In conclusion, both  $[26]\text{HCD}\cdot 4\text{H}^+$  and  $[28]\text{HCD}\cdot 2\text{H}^+$  hybrids afford two different cage-like environments (a dissymmetric

and a  $C_3$ -symmetric one) relying on the conformation of the protonated hexaphyrin cap. This allows expanded and restricted recognition to be achieved under respective kinetic and thermodynamic control. Indeed, in the case of  $[26]\text{HCD}\cdot 4\text{H}^+$ , the number of encapsulated MSA counterions and their positioning are drastically affected by a temperature controlled rectangular-to-triangular shape-shifting process of the cap. While expanded porphyrins still remain to be integrated in adaptive chemical systems, their ability to undergo spectacular conformational changes, even in triply-bridged systems, appears attractive to generate new kinds of allosteric molecular receptors and catalysts, which is in progress in our laboratories.

## References

- 1 T. W. Traut, *Allosteric Regulatory Enzymes*, Springer Science & Business Media, Boston, MA, 2008.
- 2 Selected reviews: (a) M. J. Wiestner, P. A. Ulmann and C. A. Mirkin, *Angew. Chem. Int. Ed.*, 2011, **50**, 114; (b) C. Kremer and A. Lützen, *Chem. Eur. J.*, 2013, **19**, 6162; (c) V. Blanco, D. A. Leigh and V. Marcos, *Chem. Soc. Rev.*, 2015, **44**, 5341.
- 3 S. Zarra, D. M. Wood, D. A. Roberts and J. R. Nitschke, *Chem. Soc. Rev.*, 2015, **44**, 419.
- 4 For a rare example of « bent-shape » hydrogen-bound molecular capsule, see: K. Tiefenbacher, D. Ajami and J. Rebek Jr., *Angew. Chem. Int. Ed.*, 2011, **50**, 12003.
- 5 G. Zhang and M. Mastalerz, *Chem. Soc. Rev.*, 2014, **43**, 1934.
- 6 M. Ménand, M. Sollogoub, B. Boitrel and S. Le Gac, *Angew. Chem. Int. Ed.*, 2016, **55**, 297.
- 7 Selected reviews: (a) M. Stępień, N. Sprutta and L. Latos-Grażyński, *Angew. Chem. Int. Ed.*, 2011, **50**, 4288; (b) S. Saito and A. Osuka, *Angew. Chem. Int. Ed.*, 2011, **50**, 4342.
- 8 For protonation triggered conformational changes in hexaphyrins, see: (a) T. Koide, K. Youfu, S. Saito and A. Osuka, *Chem. Commun.*, 2009, 6047; (b) S. Ishida, T. Higashino, S. Mori, H. Mori, N. Aratani, T. Tanaka, J. M. Lim, D. Kim and A. Osuka, *Angew. Chem. Int. Ed.*, 2014, **53**, 3427; (c) K. Naoda, H. Mori, J. Oh, K. H. Park, D. Kim and A. Osuka, *J. Org. Chem.*, 2015, **80**, 11726.
- 9 For protonation triggered conformational changes in other expanded porphyrins, see: (a) S. Saito, J.-Y. Shin, J. M. Lim, K. S. Kim, D. Kim and A. Osuka, *Angew. Chem. Int. Ed.*, 2008, **47**, 9657; (b) J. M. Lim, J.-Y. Shin, Y. Tanaka, S. Saito, A. Osuka and D. Kim, *J. Am. Chem. Soc.*, 2010, **132**, 3105; (c) M. Stępień, B. Szyszko and L. Latos-Grażyński, *J. Am. Chem. Soc.*, 2010, **132**, 3140.
- 10 Considering the present HCDs, “A” and “B” correspond to the  $C_6F_5$  and aryl-linker *meso*-substituents.
- 11 For a general review on chirality, see: A. Collet, J. Crassous, J.-P. Dutasta and L. Guy, *Molécules Chirales Stéréochimie et Propriétés*, EDP Sciences, CNRS Editions, 2006.
- 12 S. Guieu, E. Zaborova, Y. Blériot, G. Poli, A. Jutand, D. Madec, G. Prestat and M. Sollogoub, *Angew. Chem. Int. Ed.*, 2010, **49**, 2314.
- 13 T. Steiner, *Chem. Commun.*, 1997, 727.
- 14 For the unique X-ray structure of a protonated triangular  $[26]\text{hexaphyrin}(1.1.1.1.1.1)$ , which is unstable, see: Y.-S. Xie, K. Yamaguchi, M. Toganoh, H. Uno, M. Suzuki, S. Mori, S. Saito, A. Osuka and H. Furuta, *Angew. Chem. Int. Ed.*, 2009, **48**, 5496.
- 15 A strong deshielding of the cyclodextrin H5 protons evidences a paratropic ring current effect resulting from an antiaromatic hexaphyrin.